Available online at www.sciencedirect.com

ScienceDirect

Journal of the European Ceramic Society 31 (2011) 369–376

www.elsevier.com/locate/jeurceramsoc

Oxidation resistance of SIC–AlN ceramics coated by oxidation-assisted-pack cementation process

Giuseppe Magnani[a,*], Francesco Antolini[b], Leandro Beaulardi[b], Alida Brentari[b], Emiliano Burresi[b]

[a] *ENEA, UTTFISSM-SICCOMB, Bologna Research Center, Via dei Colli 16, 40136 Bologna, Italy*
[b] *ENEA, UTTMATF, Bologna Research Center, Via Ravegnana 186, 48018 Faenza, Italy*

Received 14 April 2010; received in revised form 6 October 2010; accepted 11 October 2010
Available online 10 November 2010

Abstract

Liquid-phase-pressureless-sintered SiC–AlN–Y_2O_3 composites were coated by means of modified pack cementation process (OXPAC, OXidation-assisted-PAck Cementation) using rare-earth oxides, RE_2O_3 (RE = Sc, Er, Sm, Lu, Ho), as reactive powders. The coatings, composed by the oxidation products of SiC, AlN and rare-earth silicates, were adherent to the substrate, without porosity and with a thickness of 10 μm. The oxidation resistance of the coated SiC–AlN–Y_2O_3 ceramics was also investigated at 1500 °C for a period of 200 h. The coated samples showed specific weight gain lower than the uncoated and pre-oxidised samples. Furthermore, the specific weight gain linearly increased with the rare-earth cationic radius.

Keywords: D. SiC; Oxidation resistance; Pack cementation; Rare-earth oxide

1. Introduction

Monolithic silicon carbide (SiC) based-ceramics are currently the primary ceramic material used in oxidising conditions at high temperature. High temperature properties of monolithic SiC ceramics or SiC-based composites have been extensively studied. In particular, several studies were focused on the properties of the solid solution silicon carbide-aluminium nitride composites (2H SiC–AlN)[1–11] displaying improved high temperature properties when SiC/AlN weight ratio is greater than 80/20 and sintering temperature above 1850 °C.[1,2]

In addition, oxidation resistance of SiC–AlN ceramics depends greatly on the sintering aid used. In fact, rare-earth oxides like Y_2O_3,[3] Er_2O_3,[4,6,8] Ho_2O_3,[4] Lu_2O_3,[4,6,7,9] Sc_2O_3,[6,9,10] Sm_2O_3,[4,5] Yb_2O_3,[4,5,11] CeO_2[4] were tested as sintering-aids for liquid-phase-pressureless-sintered (LPS) SiC–AlN ceramics and the oxidation resistance of SiC–AlN–RE_2O_3 ceramics was strongly influenced by the cationic radius of the rare-earth.[4] However, further improvements are needed to extend the lifetime of the ceramic components in oxidative and corrosive environments. An approach that has been investigated is to protect the ceramics applying an environmental barrier coating (EBC) on the surface of the material. Coating methods that have been used to produce EBCs on silicon-based ceramics include dip coating,[12] plasma spray,[13] CVD[14] and pack cementation.[15]

The pack cementation process is of particular interest because it does not require special equipment, it is a simple batch process allowing the simultaneous coating of multiple parts and it allows the formation of a uniform coating on all surfaces of simple or complex-shaped parts. In this process the part is packed in a reactive powder bed inside a container. The part is then heated to a temperature sufficient to cause a reaction between the reactive components of the powder bed and the substrate material.

The pack cementation technique was used to improve oxidation resistance of silicon nitride ceramics,[15] while it has never been used with monolithic SiC-based materials. In this work a modified pack cementation process (OXPAC, OXidation-assisted-PAck Cementation) was proposed to obtain a protective EBC on SiC–AlN–Y_2O_3 using rare-earth oxides (Er_2O_3, Ho_2O_3, Lu_2O_3, Sm_2O_3, Sc_2O_3) as reactive powders.

2. Experimental procedure

Sintered samples of SiC–AlN–Y_2O_3 (48%wt–48%wt–4%wt) were produced by means of a

---

* Corresponding author.
E-mail address: giuseppe.magnani@enea.it (G. Magnani).

0955-2219/$ – see front matter © 2010 Elsevier Ltd. All rights reserved.
doi:10.1016/j.jeurceramsoc.2010.10.015

pressureless sintering methodology based on the process already described elsewhere.[3]

Samples, characterized by dimensions of 15 mm×3 mm×3 mm, were obtained by the bulk specimens employing a diamond saw.

After grinding to reduce superficial roughness, the samples were cleaned in an ultrasonic bath and degreased washing them using acetone and ethanol. Dried samples were put inside alumina crucible completely covered by the reactive powder. Rare-earth oxide powders of Er_2O_3 (99.9% Cerac Inc., USA), Ho_2O_3 (99.9% Cerac Inc., USA), Lu_2O_3 (99.9% Cerac Inc., USA), Sm_2O_3 (99.9% Cerac Inc., USA) and Sc_2O_3 (99.0% Treibacher Industrie AG, Austria) were used for the different tests. Oxidation-assisted-pack cementation tests were carried out at 1300 °C for 5 h in flowing air in a furnace with molybdenum disilicide heating elements. After the thermal treatment, the excess of the reactive powder was removed in an ultrasonic bath, then, the coated SiC–AlN–Y_2O_3 samples were oxidised at 1500 °C over a period of 200 h in air.

The microstructures of the samples were observed using scanning electron microscopy (SEM-LEO 438 VP). Compositions were determined by EDS analysis (Oxford Link ISIS 300), while X-ray patterns (XRD) were collected with a Philips powder diffractometer with a Bragg–Brentano geometry and equipped with a copper anode operated at 40 kV and 30 mA (step 0.02°, time 6 s). The phase analysis was carried out with the PC X'pert High Score software Version 2.2a (PANalytical B.V., Almelo, The Netherlands).

3. Results and discussion

3.1. Microstructure and composition of the coating

The XRD analysis of the samples (Fig. 1) show the presence of mullite, rare-earth silicates ($RE_2Si_2O_7$, $RE_2Si_3O_9$) and α-cristobalite. The formation of these compounds on the surface of the pressureless-sintered SiC–AlN–Y_2O_3 ceramics can be ascribed to the following chemical reactions:

$$SiC_{(s)} + (3/2)O_{2(g)} \Leftrightarrow SiO_{2(s)} + CO_{(g)} \quad (1)$$

$$SiC_{(s)} + (1/2)O_{2(g)} \Leftrightarrow SiO_{(s)} + C_{(g)} \quad (2)$$

$$4AlN_{(s)} + 3O_{2(g)} \Leftrightarrow 2Al_2O_{3(s)} + 2N_{2(g)} \quad (3)$$

$$2SiO_{2(s)} + 3Al_2O_{3(s)} \Leftrightarrow 3Al_2O_3.2SiO_{2(s)} \quad (4)$$

$$2SiO_{2(s)} + RE_2O_{3(s)} \Leftrightarrow RE_2Si_2O_{7(s)} \quad (5)$$

$$3SiO_{2(s)} + RE_2O_{3(s)} \Leftrightarrow RE_2Si_3O_{9(s)} \quad (6)$$

Reactions (1) and (2) represent the passive and active oxidation of silicon carbide, respectively. Reaction (3) is the result of the oxidation of aluminium nitride, while reactions (4)–(6) lead to the formation of mullite and rare-earth silicates. The coating is therefore formed by the oxidation products of SiC and AlN (α-cristobalite and mullite) and the rare-earth silicates due to the reactions between α-cristobalite and rare-earth oxides (reactive powders). OXPAC always requires an oxidative atmosphere: the tests performed in a oxygen-free atmosphere demonstrated that the formation of the protective coating is not possible without oxygen. The SEM images of the coated samples surface, showing the morphology of the crystalline phases, are reported in Fig. 2. The coatings appear compact without porosity and well-developed crystals of rare-earth silicates are also detectable with the EDS microprobe. SEM analysis of the cross-sections allowed to evaluate the thickness of the coatings which is always less than 10 μm (Fig. 3). These images show a thin and adherent layer without porosity at the coating/substrate interface. Furthermore, a crystalline phase containing the rare-earth cation was detected in the bulk underneath the coating. This was common

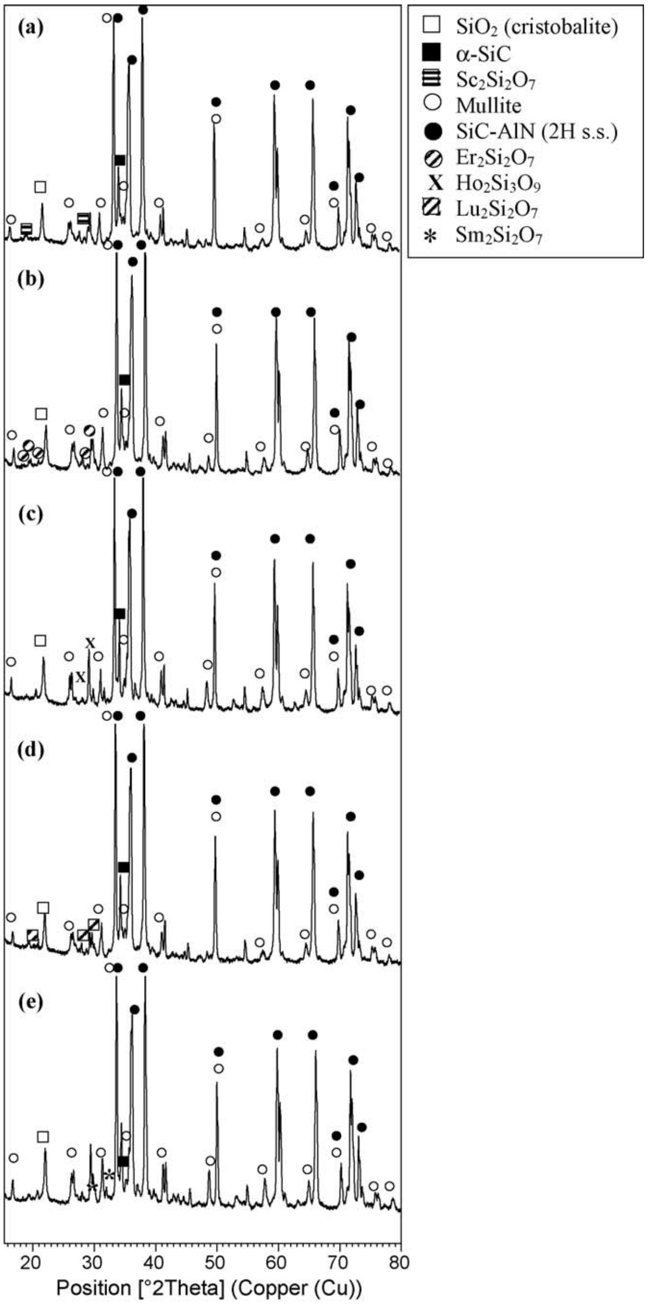

Fig. 1. XRD patterns of SiC–AlN–Y_2O_3 sintered samples coated by the OXPAC process with (a) Sc_2O_3, (b) Er_2O_3, (c) Ho_2O_3, (d) Lu_2O_3 and (e) Sm_2O_3 as reactive powders.

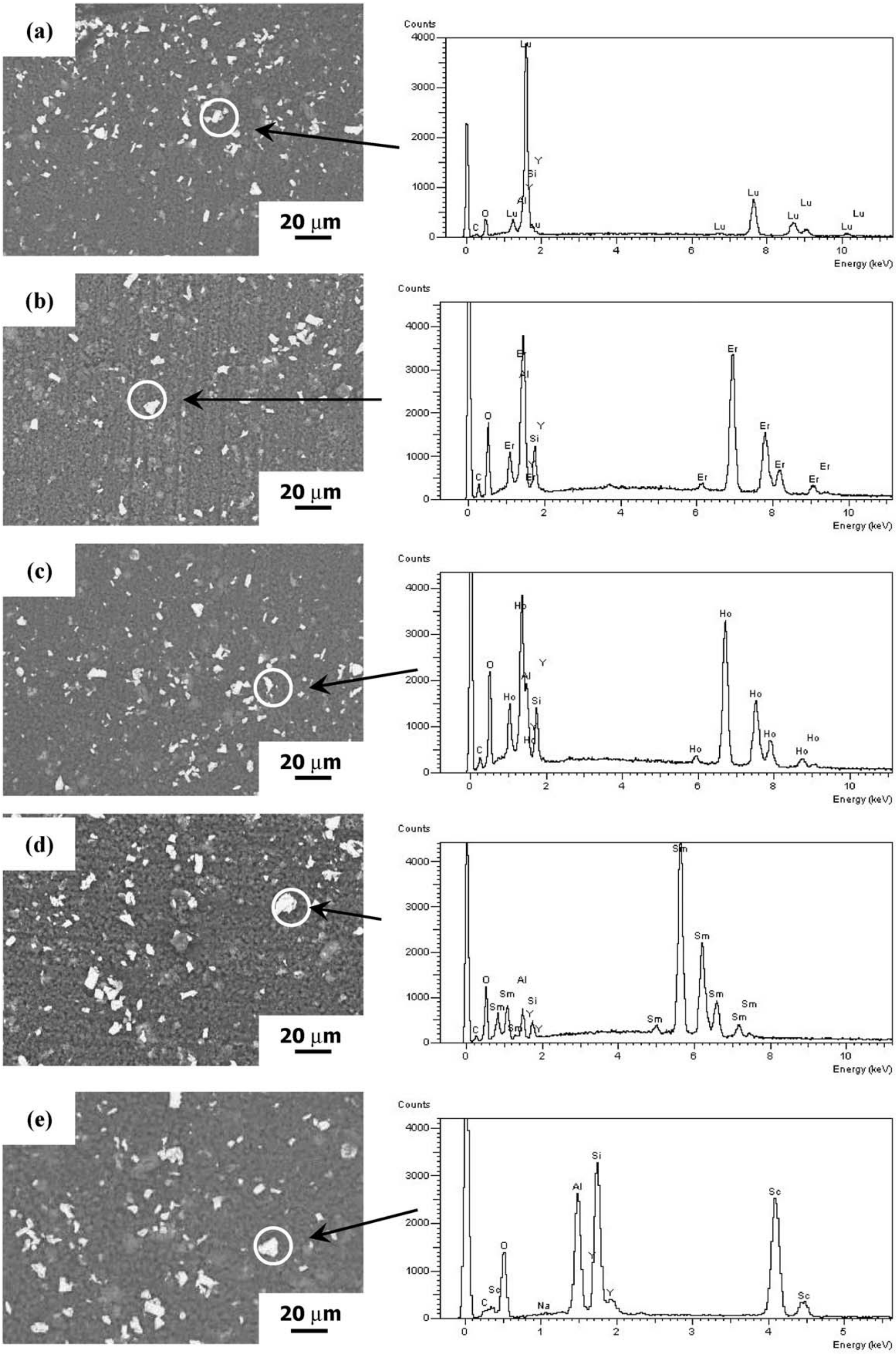

Fig. 2. SEM-EDS analysis of the surface of SiC–AlN–Y_2O_3 sintered samples coated by the OXPAC process with (a) Lu_2O_3, (b) Er_2O_3, (c) Ho_2O_3, (d) Sm_2O_3 and (e) Sc_2O_3 as reactive powders. EDS spectra are referred to the white grains shown in the corresponding image.

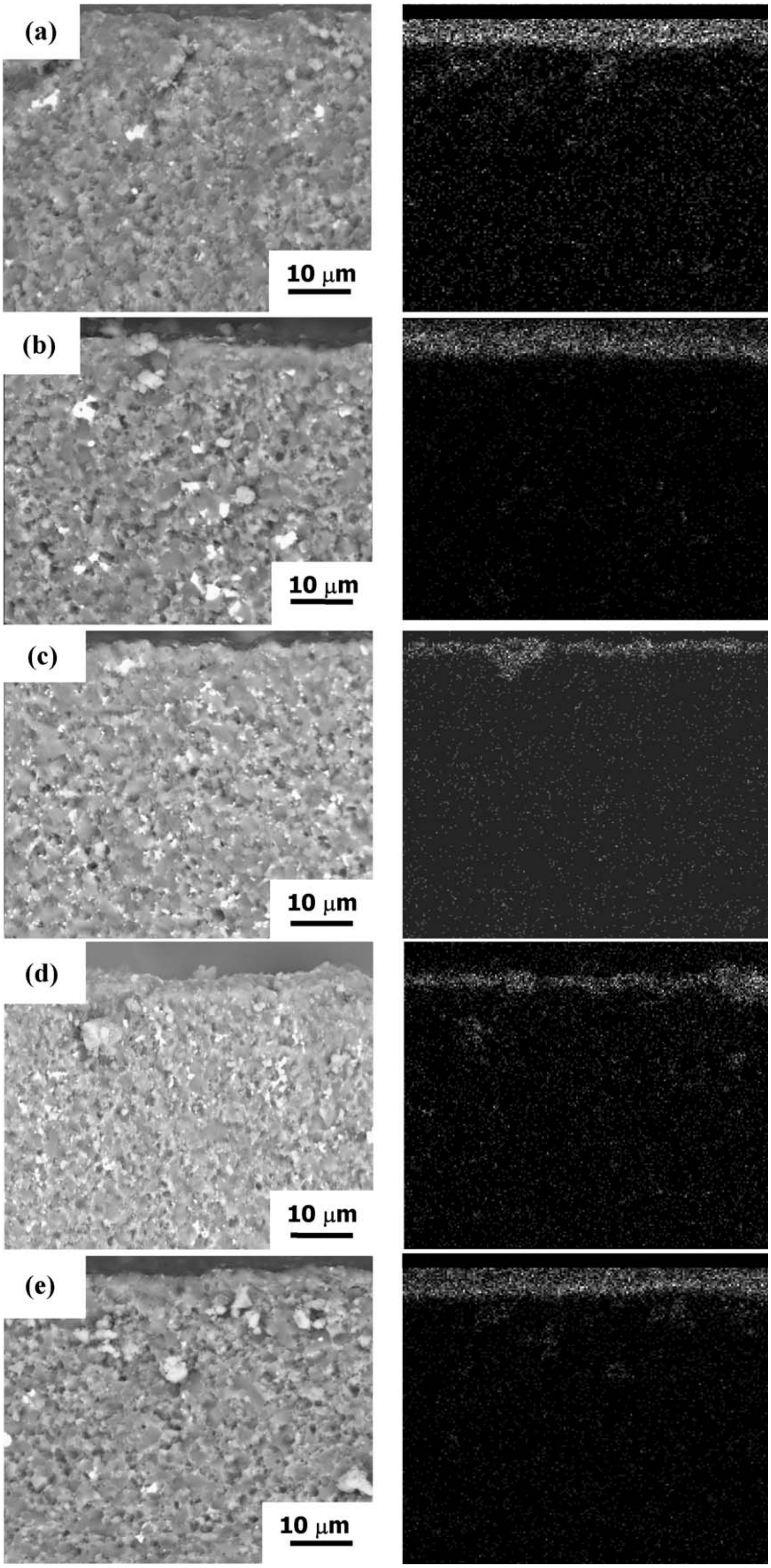

Fig. 3. SEM images and oxygen X-ray maps of the cross-section of SiC–AlN–Y_2O_3 sintered samples coated by the OXPAC process with (a) Lu_2O_3, (b) Er_2O_3, (c) Ho_2O_3, (d) Sm_2O_3 and (e) Sc_2O_3 as reactive powders.

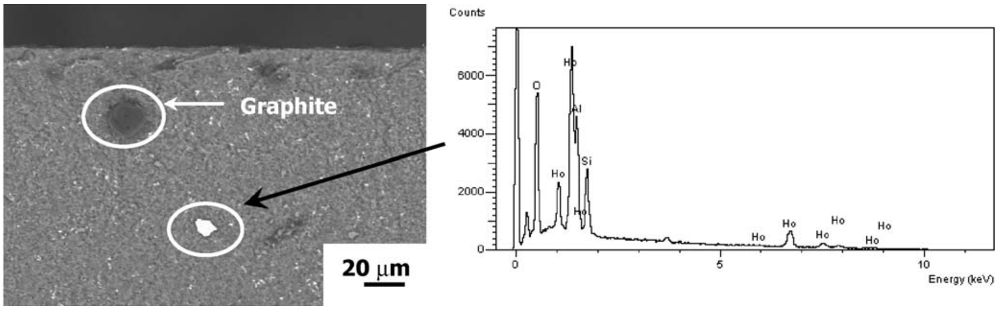

Fig. 4. SEM-EDS analysis of the cross-section of SiC–AlN–Y_2O_3 sintered sample coated by the OXPAC process with Ho_2O_3 as reactive powder.

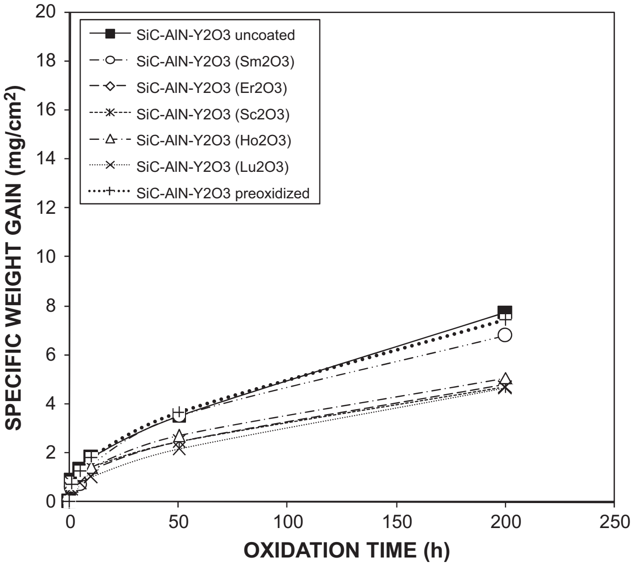

Fig. 5. Specific weight gain as function of the oxidation time for uncoated, pre-oxdised and coated SiC–AlN–Y_2O_3 ceramics ($T = 1500\,°C$).

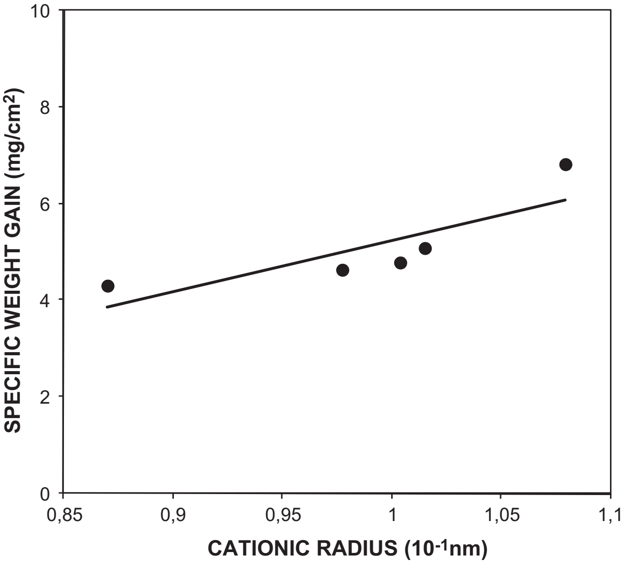

Fig. 6. Specific weight gain of the coated SiC–AlN–Y_2O_3 ceramics as function of RE^{3+} radius of the reactive powder used in the OXPAC process.

for all types of the reactive powders used in the pack cementation process and any correlation between the amount of inclusions and the rare-earth cation size has been found. The SEM image reported in Fig. 4 shows a well-developed Ho-contained grains. The EDS analysis of these grains confirmed that they are composed by holmium silicate (Fig. 4). It is likely that these grains fill the pores left by gaseous SiO, which is produced by the active oxidation of silicon carbide. In fact, in a previous paper it has already been demonstrated that the active oxidation in SiC–AlN composites shows the first effect at 1300 °C,[16] even if the effects of the passive oxidation of the SiC grains still remain with formation of SiO_2 (see Fig. 1).

Direct consequence of the active oxidation is the formation of the graphite inclusions[16]; an example of that is reported in Fig. 4 where a graphite inclusion is clearly shown. Therefore, it could be argued that the open porosity left by SiO allow the diffusion of the rare-earth oxides from reactive powder into the bulk; here they react with SiO_2 to produce rare-earth silicates.

3.2. Oxidation behaviour

The oxidation tests were performed for a period of 200 h and the weight gain per unit surface area as a function of the oxidation

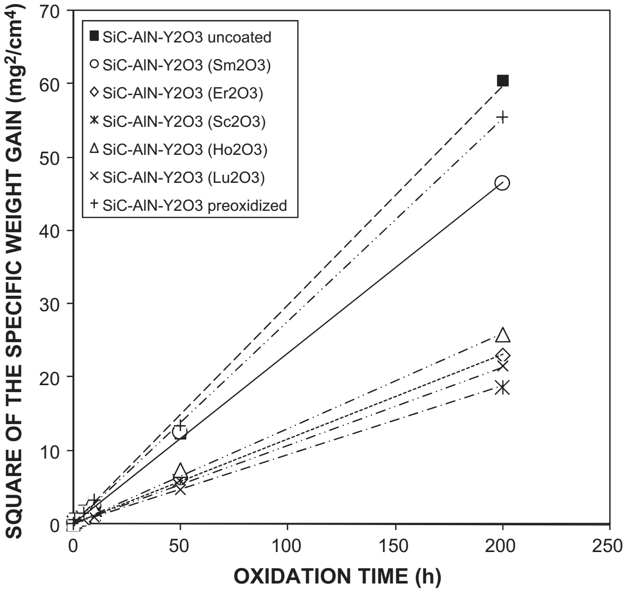

Fig. 7. Square of the specific weight gain as function of the oxidation time for uncoated, pre-oxidised and coated SiC–AlN–Y_2O_3 ceramics ($T = 1500\,°C$).

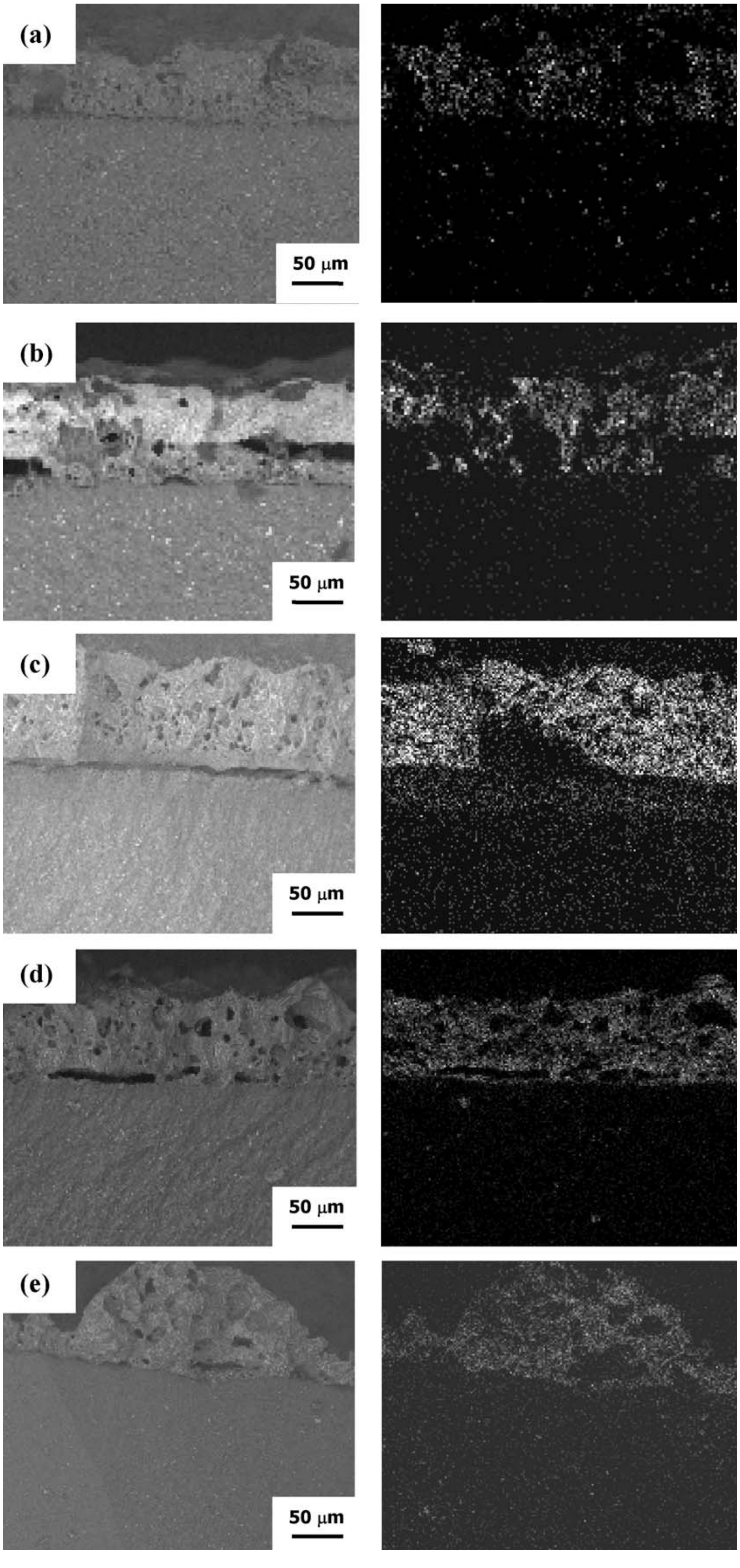

Fig. 8. SEM images and oxygen X-ray maps of the cross-section of the coated SiC–AlN–Y_2O_3 samples after oxidation at 1500 °C for 200 h with (a) Er_2O_3, (b) Lu_2O_3, (c) Ho_2O_3, (d) Sc_2O_3 and (e) Sm_2O_3 as reactive powders.

Table 1
Cationic radius of the rare-earth oxides used in the OXPAC process, specific weight gains and rate constants of the uncoated, pre-oxidised and coated SiC–AlN–Y_2O_3 ceramics after oxidation at 1500 °C for 200 h.

Substrate	Pack composition	Cationic radius of RE^{3+} (10^{-1} nm)	Specific weight gain (mg/cm^2)	Parabolic rate constant (Kg^2 m^{-4} s^{-1})
SiC–AlN–Y_2O_3	Uncoated		7.77	8.29×10^{-9}
	Pre-oxidised		7.44	7.67×10^{-9}
	Sc_2O_3	0.87	4.30	2.62×10^{-9}
	Lu_2O_3	0.977	4.64	2.97×10^{-9}
	Er_2O_3	1.004	4.79	3.21×10^{-9}
	Ho_2O_3	1.015	5.07	3.61×10^{-9}
	Sm_2O_3	1.079	6.81	6.46×10^{-9}

time at 1500 °C are reported in Fig. 5. The same oxidation tests were also carried out on the uncoated and pre-oxidised samples. This last sample was obtained after oxidation at 1300 °C for 5 h of the as-sintered SiC–AlN–Y_2O_3 sample without any reactive powder. The uncoated and pre-oxidised samples were prepared in order to evaluate the effect of the rare-earth oxides on the improvement of the oxidation resistance. In Fig. 5 it is clearly shown that the uncoated and pre-oxidised samples present the highest specific weight gains, while the coated sample with scandium oxide shows the best oxidation resistance. The oxidation resistance of the coated materials is higher than uncoated and pre-oxidised SiC–AlN–Y_2O_3 composites; it is demonstrated by the values of specific weight gains of Table 1. This effect can be attributed to the thermodynamic stability of the crystalline phases (rare-earth silicates), that minimizes the rare-earth cation diffusion.

In addition, a greater refractory nature of the amorphous grain boundary phase is normally expected for those materials sintered with the oxide additives having a smaller cationic radius.[17] The same behaviour can be expected with the ceramics coated by the oxidation-assisted-pack cementation process and containing a small amount of rare-earth silicates in the bulk. In fact, in this case it was observed that the specific weight gains of the coated specimens during oxidation were dependent on the cationic radius of the rare-earth oxide used for the modified pack cementation process (Fig. 6 and Table 1).

High temperature oxidation resistance of rare-earth silicates are well-known. In particular, scandium disilicate, $Sc_2Si_2O_7$, has already been tested in water vapour and experimental results confirmed its high corrosion resistance up to 1400 °C.[18] In this work, coated SiC–AlN–Y_2O_3 samples were simply oxidised in dry air, while future efforts will have to be focused on the study of the high temperature resistance in corrosive environments.

The oxidation always follows a parabolic rate, as the following equation:

$$\Delta W^2 = kt \tag{7}$$

where ΔW is the specific weight gain, k is the kinetic constant of parabolic oxidation and t is the oxidation time. ΔW^2 as a function of the oxidation time at 1500 °C is reported in Fig. 7. According to Eq. (7), the slope of the straight lines corresponds to parabolic oxidation rate constants.

The parabolic oxidation rate constants for each of the rare-earth oxides used in the modified-pack cementation process (as well as the values of the uncoated and pre-oxidised samples), and the total specific weight gains after 200 h are also reported in Table 1.

The parabolic oxidation behaviour of the coated ceramics indicates a diffusive process with the rate-limiting step associated with the migration of rare-earth cations (RE^{3+}) from the bulk towards the surface oxide layer.

After oxidation, surface oxide layers showed the porosity left by the gaseous products formed due to the active oxidation of SiC. The SEM micrographs and the oxygen X-ray map of the cross-section of the coated samples reported in Fig. 8 clearly illustrate the effects of reaction (2). These micrographs also show that the rare-earth silicate inclusions shown in Fig. 4 disappeared and consequently we can assume that the diffusive migration of rare-earth cations from the bulk towards the surface oxide layer is the rate-limiting step of the oxidation process.

4. Conclusions

Oxidation-assisted-pack cementation process can be used to obtain a protective coating on pressureless-sintered SiC–AlN–Y_2O_3 composites. When rare-earth oxides RE_2O_3 (RE = Er, Lu, Ho, Sm, Sc) are used as reactive powders, EBCs are composed by mullite, silica and rare-earth disilicates. Rare-earth silicates are also detected in the bulk underneath the coating due to the diffusion of the rare-earth oxides into the bulk and to the active oxidation of silicon carbide. In fact, volatile SiO causes the formation of open porosity which is filled by rare-earth oxides or graphite inclusions (by-product of the active oxidation of silicon carbide).

The coated samples show an higher oxidation resistance than uncoated and pre-oxidised ones at 1500 °C. The cationic radius of the rare-earth oxides used as reactive powders is the key factor influencing the oxidation resistance of the coated SiC–AlN–Y_2O_3 ceramics.

Oxidation always follows a parabolic rate law with migration of RE^{3+} ions from the bulk towards the surface as rate limiting step.

References

1. Zangvil A, Ruh R. Phase relationship in the silicon carbide-aluminum nitride system. *J Am Ceram Soc* 1988;**71**(10):884–90.
2. Lim CS. Effect of α-SiC on the microstructure and toughening of hot-pressed SiC–AlN solid solution. *J Mater Sci* 2000;**35**:3029–35.

3. Magnani G, Beaulardi L. Mechanical properties of pressureless sintered SiC–AlN composites obtained without sintering bed. *Ceram Eng Sci Proc* 2004;**25**(4):31–6.
4. Magnani G, Antolini F, Beaulardi L, Burresi E, Coglitore A, Mingazzini C. Sintering, high temperature strength and oxidation resistance of liquid-phase-pressureless-sintered SiC–AlN ceramics with addition of rare-earth oxides. *J Eur Ceram Soc* 2009;**29**(11):2411–7.
5. Balog M, Sedlackova K, Zifcak P, Janega J. Liquid phase sintering of SiC with rare-earth oxides. *Silikaty* 2005;**49**(4):259–62.
6. Kim YW, Chun YS, Lee SH, Park JY, Nishimura T, Mitomo M, Ryu WS. Microstructure and mechanical properties of heat-resistant silicon carbide ceramics. *Key Eng Mater* 2007:336–8, 1409–1413.
7. Biswas K, Rixecker G, Aldinger F. Effect of rare-earth cation additions on the high temperature oxidation behaviour of LPS-SiC. *Mater Sci Eng A* 2004;**374**(1–2):56–63.
8. Guo S, Hirosaki N, Tanaka H, Yamamoto Y, Nishimura T. Oxidation behaviour of liquid-phase sintered SiC with AlN and Er_2O_3 additives between 1200 °C and 1400 °C. *J Eur Ceram Soc* 2003;**23**:2023–9.
9. Choi HJ, Kim YW, Mitomo M, Nishimura T, Lee JH, Kim DY. Intergranular glassy phase free SiC ceramics retains strength at 1500 °C. *Scr Mater* 2004;**50**:1203–7.
10. Kim YW, Lee SH, Nishimura T, Mitomo M. Heat resistant silicon carbide with aluminium nitride and scandium oxide. *Acta Mater* 2005;**53**:4701–8.
11. Izhevskyi VA, Bressiani AHA, Bressiani JC. Effect of liquid phase sintering on microstructure and mechanical properties of Yb_2O_3-AlN containing SiC-based ceramics. *J Am Ceram Soc* 2005;**88**(5):1115–21.
12. Ueno S, Ohji T, Lin H-T. Designing lutetium silicate environmental barrier coatings for silicon nitride and its recession behavior in steam jets. *J Ceram Proc Res* 2006;**7**(1):20–3.
13. Bhatt RT, Choi SR, Cosgriff LM, Fox DS, Lee KN. Impact resistance of environmental barrier coated SiC/SiC composites. *Mater Sci Eng A* 2008;**486**(1–2):8–19.
14. Shah SR, Raj R. Multilayer design and evaluation of a high temperature environmental barrier coating for Si-based ceramics. *J Am Ceram Soc* 2007;**90**(2):516–22.
15. Nunn SD, Lowden RA, Montgomery FC. Producing surface coatings on silicon nitride by pack cementation. *Ceram Eng Sci Proc* 2005;**26**(3):167–72.
16. Magnani G, Brillante A, Bilotti I, Beaulardi L, Trentini E. Effects of oxidation on surface stresses and mechanical properties of liquid phase pressureless-sintered SiC–AlN–Y_2O_3 ceramics. *Mater Sci Eng A* 2008;**486**:381–8.
17. Zhiliang H, Laifei C, Litong Z, Yiguang W. Water vapor corrosion behavior of scandium silicates at 1400 °C. *J Am Ceram Soc* 2009;**92**(1):193–6.
18. Choi HJ, Lee JG, Kim YW. High temperature strength and oxidation behaviour of hot-pressed silicon nitride-disilicate ceramics. *J Mater Sci* 1997;**32**:1937–42.